Separation and Purification Technology 234 (2020) 116091

Contents lists available at ScienceDirect

Separation and Purification Technology

journal homepage: www.elsevier.com/locate/seppur

Influence of Si and Fe/Cr oxides as intermediate layers in the fabrication of supported Pd membranes

M. Maroño[a,*], G. ÓAlessandro[a], A. Morales[a], D. Martinez-Diaz[b], D. Alique[b], J.M. Sánchez[a]

[a] CIEMAT, Combustion and Gasification Division, Av. Complutense 40, 28040 Madrid, Spain
[b] Department of Chemical, Energy and Mechanical Technology, Rey Juan Carlos University, C/ Tulipán s/n, 28933 Móstoles, Madrid, Spain

A B S T R A C T

This paper presents for the first time relevant insights on the influence of tuning porous stainless steel (PSS) supports for the preparation of metallic membranes by the Electroless Pore-Plated (ELP-PP) method. Two types of oxides, used as intermediate layer between the support and the Pd layer, were deposited on raw PSS supports for reducing porosity and surface roughness. Both independent and combined routes were considered: (i) Fe_2O_3-Cr_2O_3 oxides obtained by direct calcination of the metallic support and (ii) dense and porous SiO_2 deposited by dip-coating (DC) technique. Membranes morphology (porosity and surface homogeneity) was characterized by SEM and EDX analysis and gravimetric analysis was used to calculate the total amount of Pd deposited on the external selective layer. Preliminary screening tests suggested that the combined route (calcination followed by DC of SiO_2) did not show evident beneficial effects for the preparation of Pd films by ELP-PP. Based on those results, four tubular membranes were fabricated using independent routes: one by calcination and other three by DC, including 1, 2 and 3 layers of SiO_2. The first one, including a Fe_2O_3-Cr_2O_3 oxides intermediate layer, maintained its mechanical integrity when tested up to $\Delta P = 4$ bar. On the other hand, it was observed that the use of SiO_2 intermediate layers noticeably affects the ELP-PP method. Extensive characterization of fresh and used samples has been performed in order to understand the influence of the oxides in the final preparation of a continuous and thin layer of Pd. Results obtained evidenced that the most adequate sample was the support prepared with 2 layers of SiO_2 and studies continue to improve membrane stability and to reduce thickness.

1. Introduction

Hydrogen, as one of the next generation fuels and promising energetic vector, can be generated from different renewable sources in a sustainable manner. A wide variety of production processes are available with diverse maturity grades [1], including thermochemical [2,3], electrochemical [4] and biological methods [5]. Most of the thermochemical routes produce a mixture of gases containing H_2, CO, CO_2, CH_4, H_2O and other sub-products that must be removed to obtain the H_2 purity required for its end-use (i.e. direct combustion, fuel cells or production of chemicals) [6,7].

Suitability of dense Pd-based membranes for producing highly pure hydrogen is well known since decades. Complete reviews can be found in literature, highlighting relevant milestones and the most recent advances in Pd membranes [8–10]. Together with studies on lab-scale membranes manufacturing, upscaling of fabrication processes for their use in demonstration projects and industrial applications are increasing significantly [11,12].

Despite the great advances in this field, there are still open opportunities for improving this technology, mainly directed to its commercialization. Most of the recent research lines are focused on increasing hydrogen permeability, improving the membrane resistance to poisoning or reducing membrane production costs [13,14]. Those main objectives can be achieved by improving the current membrane fabrication methods [15] and considering the use of ternary (or higher) palladium alloys to improve the properties of the selective layer [16].

Suitability of supported palladium-based membranes for their use in industrial applications is assumed due to the possibility they offer to reduce the Pd layer thickness to very low values (up to 1 μm or lower), which is essential for producing low cost and highly H_2 permeable membranes [17–19]. A supported membrane consists of a support, made of a porous material (metallic or ceramic) which provides mechanical resistance, and a thin H_2 selective layer, generally based on pure Pd or Pd-alloys, which provides the required H_2 perm-selective [20]. Usually, in case of considering metallic supports, specific pretreatments such as surface roughness smoothening or intermetallic diffusion minimization can be required. Special attention is usually paid to minimize the diffusion of metallic atoms (Ni, Fe, etc.) present in the support into the Pd layer, thereby affecting the H_2 permeance of the membrane. At temperatures close to half of the support material's melting point, metallic atoms start to acquire sufficient mobility to diffuse into adjacent layers and this is known as intermetallic diffusion. This effect has been observed in the case of Pd supported membranes at temperatures higher than 300 °C [21]. The use of different strategies can be found in literature to mitigate this effect including the formation or deposition of an intermediate layer between both PSS and Pd film

* Corresponding author.
E-mail address: marta.marono@ciemat.es (M. Maroño).

https://doi.org/10.1016/j.seppur.2019.116091
Received 18 March 2019; Received in revised form 14 September 2019; Accepted 14 September 2019
Available online 16 September 2019

Table 1
Influence of support grade on Pd layer thickness (reproduced with permission).

Support grade (μm)	Maximum pore size (μm)	Predicted Pd layer thickness (μm)	Actual Pd layer thickness (μm)
0.1	~4–5	12–15	11.7–14.3
0.2	~6–7	18–21	18.1–22.2
0.5	~11–12	24–36	24.6–33.8

[22,23]. Despite the potential benefits of using special stainless steels as supports for manufacturing Pd-based membranes, such as Hastelloy or Incoloy alloys, porous stainless-steel supports (PSS) are preferred due to their good mechanical properties, suitable corrosion resistance, lower to moderate price and easy fitting to conventional process devices. However, the low control of pore size distribution and surface roughness are the most important disadvantages of using metal supports [24]. Those properties widely depend on porous grade and manufacturer, so the selection of a particular PSS support is of key importance. Both average porosity and pore size have demonstrated to affect the minimum Pd thickness for a completely dense layer. This influence was studied in detail by Mardilovich et al. [25] who determined the required Pd layer thickness depending on the PSS support grade, as summarized in Table 1.

As showed in table 1, PSS supports with the smallest pores (grade 0.1 μm) facilitate the preparation of thinner Pd layers, although it is necessary to take into consideration that the lower the support grade, the higher the cost. Then, it is worth developing strategies for new deposition methods that can cope with supports with high media grade.

One of these strategies is based on the incorporation of intermediate layers between the metallic support and the selective Pd-based layer. Diverse metal oxides such as Fe_2O_3, Cr_2O_3, Al_2O_3, SiO_2, ZrO_2 or YSZ (Yttrium Stabilized Zirconia) can be found in literature as suitable materials for this purpose. The threefold objective of these intermediate layers includes the surface tuning (both average pore size and external roughness reduction), the improvement of adherence between both support and selective film and the reduction of the undesirable intermetallic diffusion of support elements into the selective film. For example, Fe_2O_3 and Cr_2O_3 oxides can be easily generated on the surface of PSS supports by direct calcination in air as reported by Huang et al. [26] and Furones et al. [27] in previous works. However, in those cases, only a slight modification of surface roughness is achieved and the reduction of the original biggest pores is limited in comparison to the incorporation of other materials, so the effectiveness against metal inter-diffusion could be limited, especially in case of operating during long periods at high temperatures (> 500 °C).

The use of other ceramic materials as intermediate layer such as ZrO_2 [28], YSZ [29] or SiO_2 [30,31] can be also easily found in literature. Particularly, suitability of SiO_2 has been recently used for repairing pinholes in Pd based membranes at a very low cost [32] or for its combination with Pd in mixed matrix structures [33].

On the other hand, a wide variety of technologies is available for incorporating the Pd-selective layer. They include Electroless Plating (ELP) [12], Physical Vapor Deposition (PVD) [31], Chemical Vapor Deposition (CVD) [32] or dip-coating technique (DC), less frequently used in the membranes fabrication field, but widely employed in applications where the preparation of very thin layers of materials is required [30,33]. The dip-coating alternative (DC) is especially interesting for thin film deposition because it presents important advantages compared to the state-of-the-art methods, such as lower capital costs, accurate control of film thickness and alloy composition, high reproducibility and good homogeneity for thin films [34]. Additionally, the high stability of the solution for long periods and the ability to recover the unused solution minimize the production of wastes [35]. This is of key importance because reducing metal losses is crucial for Pd-based membranes industrial production and cost viability. For example, stable solutions of different oxides and palladium at room temperature had been patented, being demonstrated their use for more than six months without any sign of degradation [36].

The microstructure of the H_2 selective layer, which strongly depends on fabrication technology, requires special attention due to its fundamental role in hydrogen permeability, selectivity and thermal stability [37]. Among all diverse preparation methods mentioned above, ELP alternative is the most preferred one due to its simplicity, possibility to be easily scaled-up and the good properties of deposits in terms of homogeneity and adherence [16]. However, some developments are still in progress, mainly focused on the modification of bath composition or dosage of reactants [38,39]. In this context, the Electroless Pore-Plating alternative (ELP-PP) has recently exhibited a great potential to ensure good adherence of the Pd layer and to guarantee complete absence of defects in the selective film [40,41]. This method, based on feeding both palladium source and reducing agent solutions from opposite sides of the porous support, ensures the formation of a dense and continuous Pd layer on the surface of supports with the minimum palladium thickness required for a complete coating without pinholes and defects. The application of ELP-PP method showed that an external Pd film was also deposited besides the pore-filling, suggesting that support characteristics are critical to define the palladium distribution in the final membranes [42].

The current research is based on unravelling the effect of porous stainless steel supports tuning on the preparation of Pd-based membranes by the new electroless pore-plated methodology. Diverse intermediate layers have been considered in both independent and combined routes for the study: (i) Fe_2O_3-Cr_2O_3 oxides by direct calcination and (ii) SiO_2 by sol-gel and dip-coating procedures. Characterization of the membranes has provided significant insights on the influence and benefits of each type of oxide in the final deposition of the Pd selective layer.

2. Experimental

2.1. Supports configuration and preliminary preparation

In this work, porous stainless steel 316L supports with different media grades, purchased to Mott Metallurgical, were used to prepare the membranes. A media grade of 0.2 μm was used in flat geometry with original dimensions of 25x25 cm, while a media grade of 0.1 μm was considered for cylindrical geometry with 25 cm in length and outer diameter of around 1.8 cm (1/2 in.). The raw supports were cut to obtain the adequate dimensions to be coupled into the available permeation equipment, obtaining discs with diameter 4 cm and tubular membranes pieces of 5 cm length that were additionally welded to dense SS316L tubes in both extremes making a total length of 15 cm. For the last case, one end was closed and adequate fittings were welded to the other extreme of the support to facilitate its connection into the permeation equipment for ensuring a good sealing. Both final supports and the membrane housing for each described geometry, flat and tubular, are shown in Fig. 1.

Once the supports were prepared, an initial cleaning was carried out for minimizing the possible effect of surface impurities generated during fabrication, transport or storage. Each sample was cleaned by successive ultrasonically washing in ethanol and acetone for 2 h with a final drying step at 80 °C for 4 h. Cleanness of the supports was checked by surface EDX analysis in a scanning electron microscope prior to continue the preparation process of the membranes.

2.2. Development of intermediate layers

As we have previously indicated, two different materials have been considered to be used as intermediate layers for the preparation of the membranes: Fe_2O_3-Cr_2O_3 oxides and SiO_2. The first alternative has been achieved by direct calcination of raw PSS supports, while the second

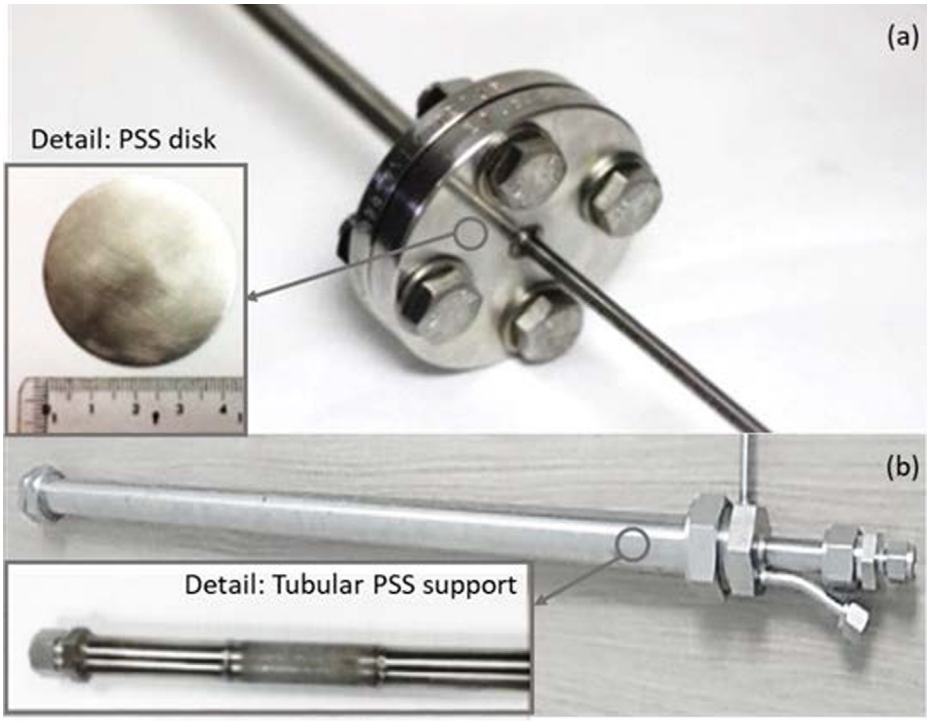

Fig. 1. PSS supports and membrane housing: flat (a) and tubular (b) geometries.

one has been prepared by sol-gel and dip-coating processes. These options have been evaluated independently, being generated directly on a raw support each particular intermediate layer and combining both of them in the same sample to take advantages of benefits given by each material. In the last case, the based Fe-Cr oxides intermediate layer was firstly incorporated on the raw PSS support, followed by a silica layer on the top surface.

Here, a brief description for the experimental procedures followed to prepare each intermediate layer has been included.

2.2.1. Fe-Cr oxides intermediate layer

The generation of the iron-chromium oxides as intermediate layer has been carried out by in-situ oxidation of the PSS raw supports in air atmosphere and high temperature. A detailed effect of combined PSS support media grade and calcination conditions on original surface modification and permeation behavior was previously published by Furones et al. elsewhere [27]. Based on the results obtained in the aforementioned study, a calcination temperature of 600 °C for 12 h was used in the present work to generate the metal oxides with heating and cooling ramp rates of 1.8 °C min^{-1} onto PSS raw supports with tubular geometry.

2.2.2. Silica intermediate layer

The silica intermediate layers have been obtained by using a sol-gel procedure followed by dip-coating. Two different oxide precursors have been investigated: dense and porous SiO_2 particles. First screening tests were carried out on flat supports by depositing 1, 2 and 3 layers of both types of silicon oxide precursors and the most promising one was then used for preparing the tubular membranes.

Sol-gel dense silica precursor solution was prepared using tetraethylortosilicate (TEOS) as silica precursor alcoxide, hydrolyzed with water and catalyzed with chloride acid. During this process, absolute ethanol was used as solvent. Dense silica films were prepared using TEOS:water:ethanol:HCl in a molar ratio of 1:5.1:48:0.08. In order to prepare porous silica layers, porogen Triton X-100 was added to the dense precursor solution [43]. After that, dense and porous silica layers have been deposited onto the supports at withdrawal rate of 25 cm min^{-1}, being finally cured in an oven at 500 °C for 1 h.

2.3. Incorporation of H_2 selective layer: Palladium deposition

The principal method considered in this work for the incorporation of the H_2-selective layer has been ELP-PP, recently published as a very attractive alternative and still under study for optimization under diverse support characteristics [40]. Additionally, Pd was also directly painted on some modified supports in order to analyze in a quick test the influence of each intermediate layer (Fe-Cr oxides or SiO_2) on metal adherence and continuity. The painting solution was prepared by dissolving palladium chloride in a mixture of water and hydrochloride acid and adding 2-(2-aminoethylamino)ethanol as complexing agent until complete solution discoloration [36]. The substrate has first heated up to 100 °C and painted ten times with the prepared solution. Finally, the painted layer has been cured in an oven at 500 °C for 1 h to obtain the final palladium coating.

As detailed in the discussion section, those preliminary experiments evidenced that combined incorporation of Fe and Cr oxides and SiO_2 as intermediate layers did not improve the subsequent Pd selective layer deposition. Therefore, four different tubular membranes were prepared in this work, where one of the supports was modified by calcination while the other three were prepared by incorporating 1, 2 and 3 layers of dense SiO_2 by dip-coating, accordingly to the procedures previously described.

The Pd film for all these tubular membranes was prepared, as mentioned at the beginning of this section, by electroless pore-plating (ELP-PP) following the experimental procedure thoroughly described elsewhere [40]. This method can be summarized in two consecutive steps: i) support activation and ii) film conformation. The first step is required to generate an homogeneous distribution of initial Pd nuclei around the support to ensure good adherence and homogeneity of the metal film, especially near the porous areas. These initial nuclei are generated by direct reduction of an acidic $PdCl_2$ solution (0.1 g/L) with diluted N_2H_4 0.2 M in ammonia (2 M) at room temperature for 2 h. After rinsing the activated supports in deionized water and drying overnight at 110 °C, the deposition of the Pd film is initiated. For this

purpose, both metal source and reducing solutions are fed from opposite sides of the activated supports. Thus, the chemical reaction is mainly produced around the porous areas, where new metal deposits can be easily attached to the first nuclei, progressively increasing the metal amount due to the autocatalytic property of palladium for its own reduction. In general, the composition and concentration of reducing solution from the previous activation process is maintained during this step (otherwise, it will be clearly indicated in the results section), while the metal source is formed by $PdCl_2$ (5.4 g/L), EDTA (70 g/L) and NH_4OH (390 mL//L). The ratio between both solutions is keeping on $V_{ELP\text{-}Pd}$ / $V_{reducing}$ ≈ 12, while around 2.5 mL of the metal source solution is used per cm^2 of membrane area in all cases. Each deposition cycle is carried out at 60 °C for 2 h, being repeated with intermediate washing in deionized water and drying overnight (110 °C) up to the weight gain becomes negligible. This fact reflects the impossibility of direct contact between both solutions and, consequently, the generation of a fully dense Pd film.

2.4. Membrane characterization

2.4.1. Membrane morphology

All samples were completely characterized, before and after incorporation of the palladium film, in terms of external morphology and composition. Scanning Electron Microscopy (Hitachi-S-2500 and Philips XL-30 microscopes equipped with an Electron Dispersed X-Ray detector) and Optical Profiler from Zeta Instrument (model Zeta-20) were used to determine porosity and homogeneity or external roughness and related parameters, respectively. Moreover, the total amount of palladium incorporated by ELP-PP was determined by gravimetric analysis with an electronic balance Kern & Sohn ABS-4 (detection limit of 1.0 10^{-4} g). Those values were used to estimate an average palladium thickness for each membrane.

2.4.2. Permeation behavior

Prior to determine any permeation capacity at usual operating temperatures (> 300 °C), the integrity of the membranes was preliminary checked by performing leak tests in N_2 at pressures up to 6 bar by using a device designed *ad hoc* (based on the "water rising test" of F. Guazzone [44]) and illustrated in Fig. 2.

Once the membrane integrity at room temperature has been ensured, the performance of the membranes prepared in this work was tested at higher temperatures in a bench-scale plant, described in detail elsewhere [45,46]. In this case, new membrane housings were fabricated *ad hoc* and placed in the above-mentioned pilot plant for membrane testing. This facility can treat up to 2 Nm^3/h of gas at 600 °C and a maximum pressure of 20 bar. In this work, hydrogen permeability was tested for both pure gases and diverse binary H_2/N_2 mixtures (with volumetric composition of 70/30 and 50/50%), maintaining constant 1 $NL{\cdot}h^{-1}$ as total gas flowrate. All permeation tests were performed at pressure differences of 4 bar, keeping permeation side at atmospheric pressure, and 400 °C with a temperature ramp of 10 °C min^{-1} for heating up and cooling down the reactor. Besides the permeate flowrate, also hydrogen content was continuously measured by using a micro-chromatograph VARIAN 490 equipped with a MS column and a thermal conductivity detector. These data were used to determine the H_2 selectivity of membranes when feeding binary H_2/N_2 mixtures.

The equation derived from Fick's and Sieverts' laws [47] was used for all permeability calculations (Eq.1), where J is the hydrogen flux through the composite membrane (mol/m^2 s), θ is the hydrogen permeability (mol/m s $Pa^{0.5}$), l is the palladium layer thickness (m), and $P_{H2,ret}$ and $P_{H2,perm}$ are the hydrogen partial pressure at the interface in the retentate (*ret*) or permeate (*perm*) sides (Pa), respectively.

$$J = \frac{\varnothing}{l}\left(P_{H2,ret}^{0.5} - P_{H2,perm}^{0.5}\right) \quad (1)$$

The exponent for hydrogen partial pressures in permeate and retentate interfaces considered in this equation, taking a value of 0.5, is only valid when bulk diffusion is the limiting step for the overall permeation process. Thus, Eq. (1) is usually reported for supported membranes when the resistance in the porous support can be neglected. Otherwise, in case of becoming relevant other phenomena such as Knudsen diffusion or concentration-polarization, a modification of the theoretical exponent of the Sieverts' law to an empirical one ($0.5 < n < 1$) is reported in the literature [40].

Other important parameter to evaluate the permeation behavior of palladium membranes is the H_2 selectivity or H_2 separation factor (α). The general expression that is frequently used to determine its value is described in Eq. (2), where y_{H2} and y_i are the permeate molar fractions of H_2 and other species (N_2 in this case), respectively, and x_{H2} and x_i the equivalent retentate molar fractions.

$$\alpha = \frac{y_{H2}/y_i}{x_{H2}/x_i} \quad (2)$$

3. Results and discussion

3.1. Support modification: Tuning surface properties with intermediate layers

As it has been previously described in the experimental section, two different approaches were considered in this work for tuning the surface properties of the original PSS supports. Different membranes were

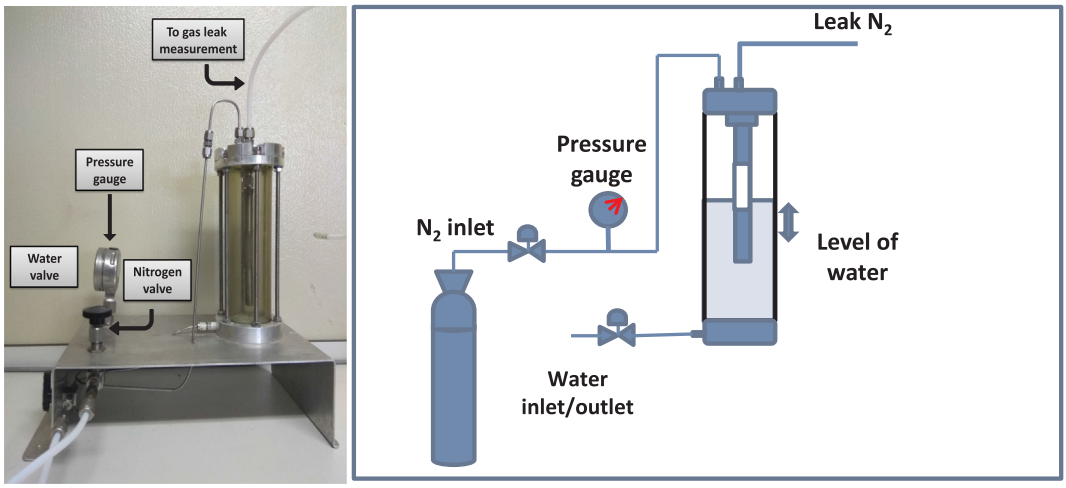

Fig. 2. Experimental device for determining the membranes integrity through leak tests.

obtained by incorporation of diverse intermediate layers: Fe and Cr oxides generated by direct oxidation of the support and SiO_2-based layer prepared by sol-gel and deposited by dip-coating techniques. Additionally, in order to check possible synergies between both approaches, the combination of PSS calcination and subsequent incorporation of a SiO_2 intermediate barrier was also investigated. Thus, two different samples were prepared with SiO_2, considering both raw PSS and calcined supports, and painting a Pd top layer. The aim of this study is to provide some insights, by simple optical microscopy, on the suitability of the proposed methods for obtaining continuous Pd layers. The first alternative, based on direct calcination of PSS support in atmospheric air, has been deeply described and optimized in a previous study [27], in which the generation of Fe-Cr oxides intermediate barrier at diverse conditions were widely discussed. Based on those results, the most favorable conditions (T = 600 °C, t = 12 h) were adopted here for preparing tubular membranes with a total length of 15 cm (5 cm of active membrane area with two dense tubes welded on both extremes) instead of a total length of 3 cm that were considered in previous works.

The second one, based on the incorporation of a SiO_2 intermediate layer by sol-gel and dip-coating techniques, has been also considered in this work. This material has been taken into consideration as a suitable inter-diffusion barrier between both PSS support and Pd film, being considerably cheaper than other alternatives typically considered in the literature [18,48]. Two different types of materials were investigated to obtain this intermediate layer: dense and porous SiO_2. While cylindrical geometry was directly used for the Fe_2O_3-Cr_2O_3 intermediate layer, in this case, a preliminary screening test was carried out on planar disc to analyze the adherence and the surface modification reached after depositing 1, 2 and 3 layers of dense and porous SiO_2.

Fig. 3 shows the SEM images of the external surface obtained by the modification of PSS discs under diverse conditions. As it can be seen in Fig. 3, an increase in the number of incorporated layers by dip-coating resulted in a greater modification of the support surface. In case of using dense SiO_2, pore filling can be easily observed, as well as the typical cracks generated when silica material is subjected to heat treatment (Fig. 3, images a, b and c placed in the upper row). Here, it is also clear that pore filling increased with the increasing number of layers incorporated by dip-coating. The material is added in the deeper

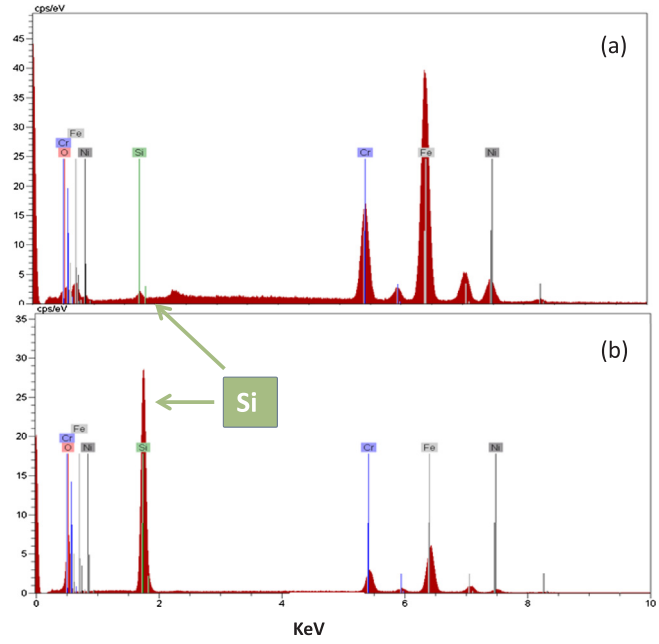

Fig. 4. EDX analysis after adherence testing for modified PSS supports with 3 layers of: (a) porous SiO_2 and (b) dense SiO_2.

areas of pores and the progressive filling seems to derive into a smoother surface. On the other hand, the incorporation of porous SiO_2, despite showing a similar effect of increasing pores filling with the increasing of the number of layers, resulted in a layer with the appearance of a veil (less consolidated material), suggesting possible problems of adherence.

In order to elucidate these possible problems of adherence between SiO_2 intermediate layers and PSS supports, it was tested for all samples by immersing them in an ethanol ultrasonic bath at room temperature for 2 min. All the samples were analyzed by EDX before and after the treatment to compare the persistence of the silica layer. A good integrity of dense SiO_2 intermediate layers was observed after the

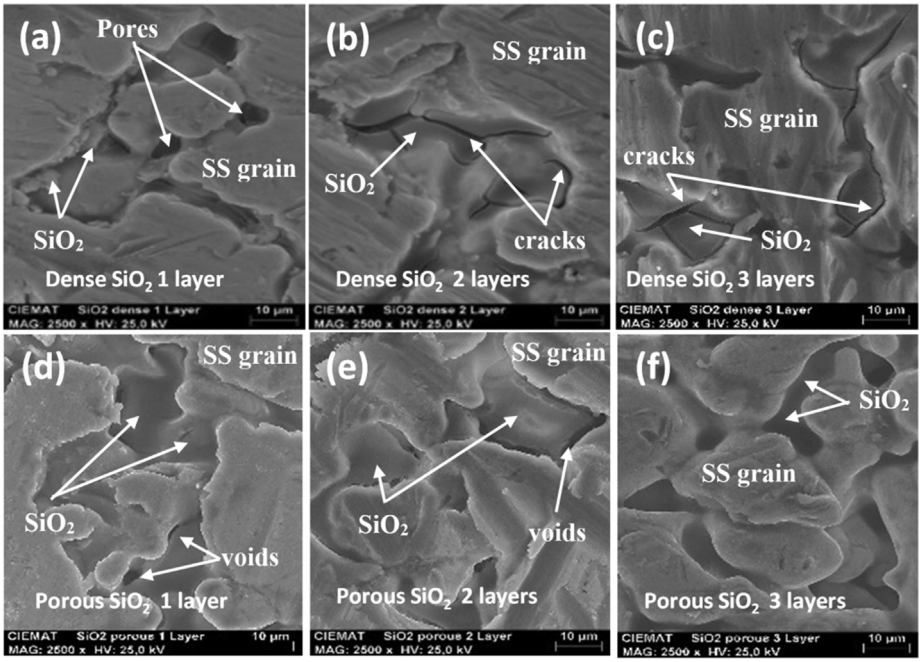

Fig. 3. External surface achieved with diverse SiO_2 intermediate barriers by using 1, 2, and 3 layers: dense SiO_2 (upper row; images a, b and c) and porous SiO_2 (lower row, images d, e and f).

treatment, independently of the number of incorporated layers, while a release of porous SiO_2 from the support at analogous conditions was observed, evidencing an immediate loss of adherence. In fact, this effect was almost inmediate when the modified supports were introduced into the bath, even for the samples including 3 layers of porous SiO_2. Fig. 4 collects the EDX analysis performed to study the adherence of the intermediate layer just after the treatment for the samples with the greatest amount of SiO_2 (3 layers). As it can be observed in Fig. 4, only supports modified with dense SiO_2 maintain the intermediate layer, resulting in the detection of the corresponding signal around 1.75 keV. Although this research is still in progress to improve the layer resistance in case of using porous SiO_2, the non-porous material has been selected here to prepare the ELP-PP membranes by incorporating this SiO_2 intermediate layer on the cylindrical supports.

Some additional experiments were also performed to analyze the convenience of a support pre-calcination before incorporating the intermediate SiO_2 layer. This alternative could improve the mechanical properties of the membrane or the adherence between layers. In this context, two different samples were prepared incorporating three layers of dense SiO_2 by dip-coating on raw and pre-calcined PSS discs. Both pieces were finally covered by a Pd film painting them directly with a Pd solution to evaluate the easiness of the modified surfaces to be covered. These samples were analysed by optical and electron scanning microscopy, collecting the generated images in Fig. 5. At this figure can be observed a greater modification with SiO_2 particles in case of avoiding the previous calcination of the raw support, being most of the internal PSS pores with the ceramic material. Moreover, in this case the external surface obtained after the modification seems to be smoother and better covered by the palladium.

Both supports were then analysed by EDX. Although the presence of Fe and Cr oxides could not be clearly identified in the calcined support in this case, their presence has been demonstrated in previous studies performed under analogous conditions [27] and for different PSS

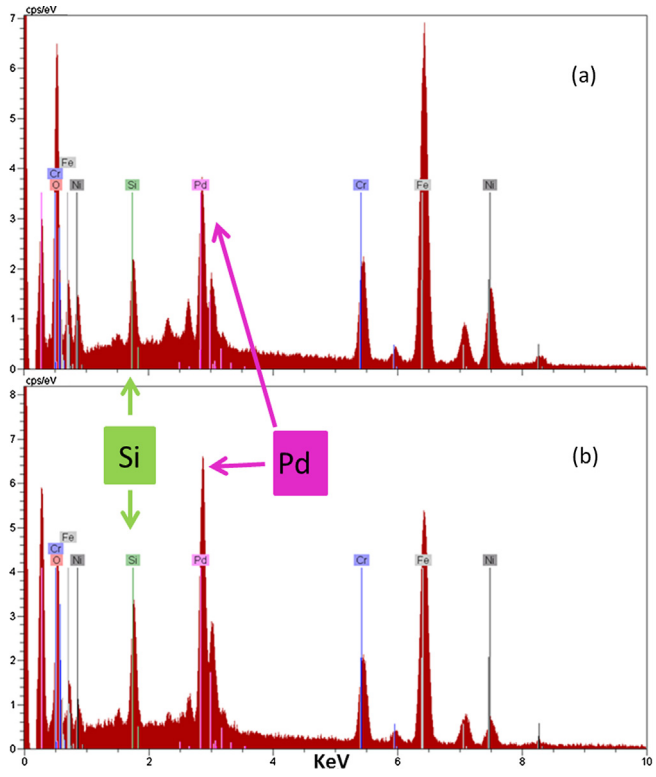

Fig. 6. EDX analysis of outer surface of modified supports by incorporation of 3 SiO_2 layers and a top film of Pd with (a) and without (b) a prealcination treatment.

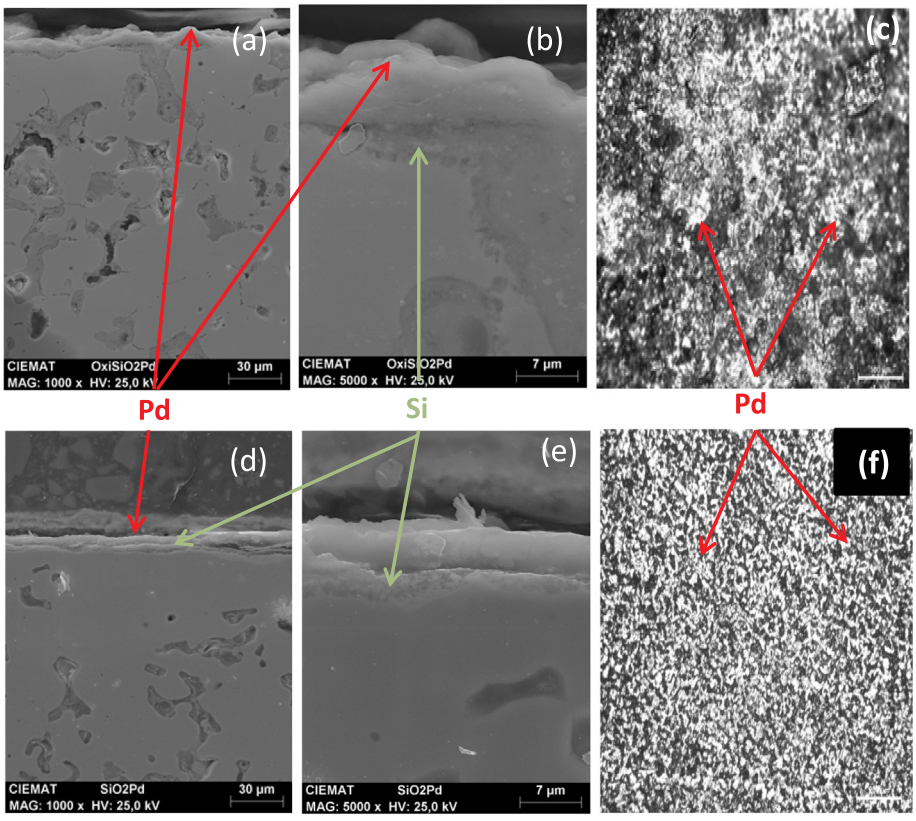

Fig. 5. Micrographs obtained by optical and electron microscopy for modified supports by incorporation of 3 SiO2 layers and a top film of Pd with (a, b, and c) and without (d, e and f) a prealcination treatment.

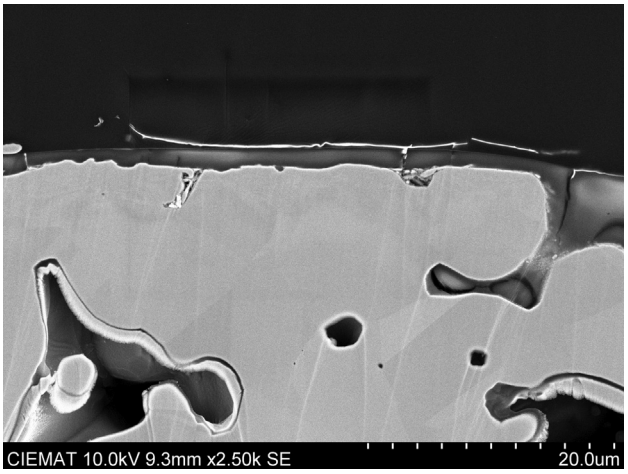

Fig. 7. Cross-section of planar membrane by Ion milling: SiO_2 and Pd layers.

supports [49–51]. In our case, the layer of oxides formed during calcination seemed to prevent a complete filling of the internal pores of the support during the subsequent dip-coating of SiO_2. The presence of an external oxide layer on the support surface might have reduced the homogeneity of the SiO_2 layer and, consequently, affected negatively the final Pd adherence. Accordingly to the EDX analysis, more intense signals for both, SiO_2 and Pd, could be found on the external surface of the non pre-calcined sample (see Fig. 6), suggesting that this pre-treatment has not an evident beneficial effect for the subsequent deposition of SiO_2 intermediate layers and, therefore, the final Pd-membrane preparation.

In order to elucidate if a continuous layer of SiO_2 could be formed on top of the metallic support, the planar membrane prepared by direct deposition of SiO_2 without pre-calcination (see picture f in Fig. 5) was analyzed by ion milling technique. Fig. 7 shows that SiO_2 not only has entered and filled the pores of the support but also has formed a continuous layer on top of the surface. A very thin although not continuous layer of Pd can be also seen in the picture (around 0,5 μm) which demonstrates that Pd layer is adherent to SiO_2 layer and can provide a suitable support to be used in the preparation of tubular membranes by ELP-PP.

Based on these preliminary results, it was decided to continue with the work using separately both modified supports (by calcination and incorporation of SiO_2 intermediate layer) and to investigate their influence on the ELP-PP method.

As it has been previously indicated, three intermediate layers based on dense SiO_2 material have been developed by sol-gel and dip-coating techniques over tubular supports. Fig. 8 shows the external surface morphology obtained by SEM, being possible to distinguish the SS grains of the support independently of the number of recurrences performed during the SiO_2 dip-coating. It suggests the preferential incorporation of SiO_2 particles inside the pores, at least near the external surface. In fact, the covering of the PSS external pores becomes greater

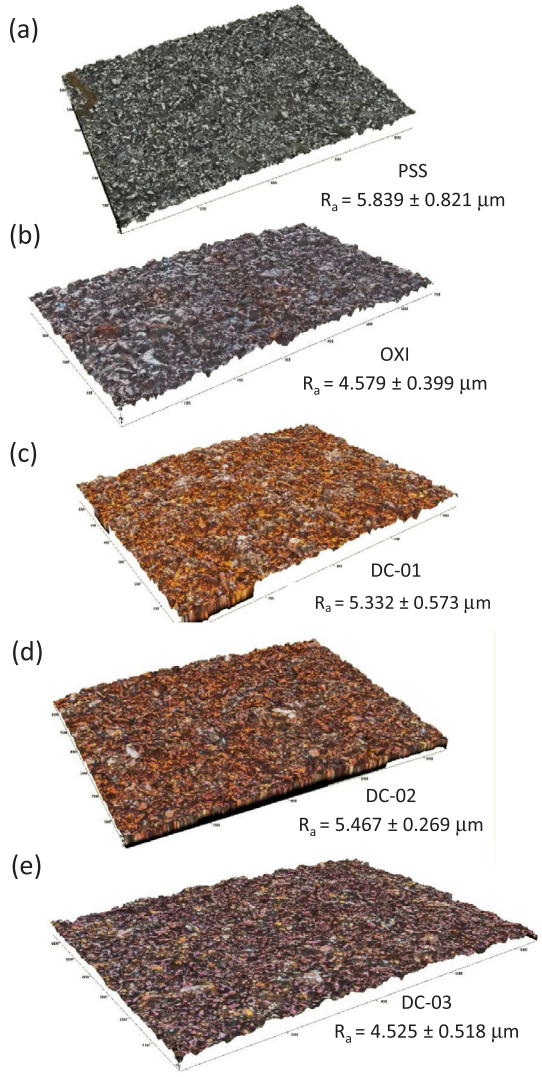

Fig. 9. Surface roughness analysis of original PSS (a) and modified supports by the incorporation of: Fe-Cr oxides (b) and 1 (c), 2 (d) or 3 (e) layers of dense SiO_2 intermediate layers.

as increasing from 1 to 3 the number of dip-coating cycles. However, the quantification of this effect on the original PSS morphology is quite difficult to analyze, requiring an additional characterization.

In order to analyze the modification of the support surface after the incorporation of these SiO_2 intermediate layers, the roughness of the new surfaces was also determined by an optical profiler (details can be seen in the experimental section). As it has been previously discussed, the silica was incorporated preferentially into the biggest pores of the support, trying to form a continuous layer onto the external surface as usually done for most of other intermediate layers reported in literature

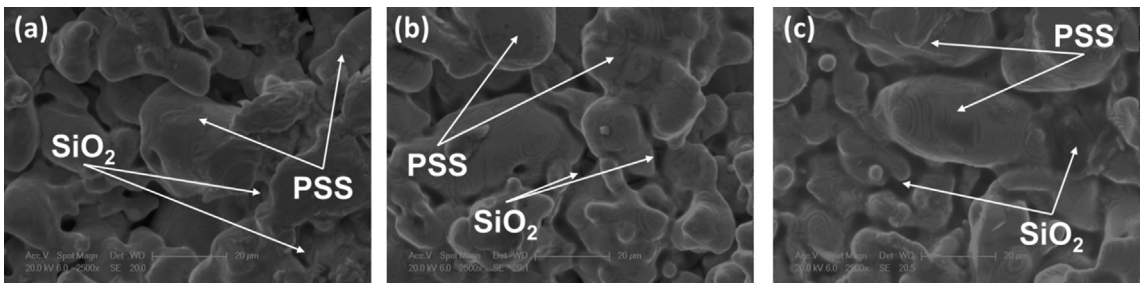

Fig. 8. SEM images for tubular PSS supports modified with dense SiO_2 by applying: (a) 1, (b) 2 and (c) 3 dip-coating cycles.

[52–54]. However, it was quite difficult to determine accurately the variation of the pore size distribution just from SEM images. Thus, the roughness values have been also calculated from profiler analysis and selected to compare the diverse grade of modification achieved at different conditions here presented. Additionally, reference roughness values for raw PSS and oxidized supports have been also included for comparison. Fig. 9 collects all these data together with the 3D recreation of the surface. At this point, it is important to emphasize that these analyses need to be carefully performed due to the curvature of the cylindrical support and the resulting values here presented are an average calculation from data collected along 5 different lines for each sample. From these results, it can be extracted that the calcination in air of the supports at 600 °C for 12 h causes an original roughness reduction of around 20%, similar to the calculated in case of using 3 layers of dense SiO_2 by dip-coating (DC-03). The other samples maintain similar roughness values, being only slightly lower than the original support. Thus, it is impossible to discern if the change is produced by the incorporation of the intermediate layer or simply it is due to the intrinsic error of measurement.

3.2. Pd deposition by ELP-PP on modified supports

The next step followed for the preparation of the membranes was the incorporation of palladium as selective layer. In this work, the Pd deposition has been carried out by the novel ELP-PP method, still under development, and never used before on PSS supports modified with a SiO_2 intermediate layer. As it has been previously indicated, the membrane conformation was carried out for tubular PSS supports (total length of 15 cm with around a third part as active permeable area), including intermediate layers formed by Fe-Cr oxides (direct calcination in air) and dense SiO_2 (dip-coating of 1, 2 and 3 layers). These membranes were denoted as OXI-Pd or DC-xx-Pd, respectively, being xx the number of dip-coating cycles carried out to incorporate the SiO_2 intermediate layer (main parameters summarized in Table 2).

Fig. 10 shows SEM images of external surface and cross-section for OXI-Pd sample, prepared in similar conditions and previously reported elsewhere [40], but increasing around 2 times the total membrane length. The amount of hydrazine solution used for the membrane preparation was always the available volume in the lumen of the tubular PSS support, while the required volume for the Pd source solution was the minimum one that ensures a complete immersion of the sample during the process. Then, considering the dimensions of the new membrane and an unique container for the preparation of all the membranes, the ratio between Pd-source and reducing agent solutions was decreased up to $V_{ELP\text{-}Pd}/V_{reducing} \approx 12$ (instead of the previous value ≈ 30 used for supports with 3 cm in length). In this manner, 2.5 mL of Pd-source solution were spent per cm^2 of membrane area. Under these conditions, results similar to those previously reported were obtained, achieving a continuous selective layer with good homogeneity, negligible porosity, average roughness around 1.500 µm and 10–15 µm in thickness. It is also important to emphasize that no significant differences could be appreciate along the total length of the membrane (images not presented here). Moreover, EDX analysis evidenced surface palladium content near 91%, balanced with carbon up to 100%, as it is usual in Pd films generated from solutions containing EDTA.

The results obtained showed that the total amount of SiO_2 deposited in the intermediate layer clearly affects the palladium plating process when preparing ELP-PP membranes onto modified supports with SiO_2. Previous works demonstrated that an hydrazine concentration of around 0.2 M was the most suitable for optimize the incorporation of Pd by ELP-PP on PSS supports [41]. However, the presence of an increasing amount of SiO_2 material into the PSS pores turns the contact between the plating solutions (both, Pd source and hydrazine) progressively more difficult. Thus, it was necessary to increase the concentration of hydrazine until the chemical reaction took place, detected by the presence of N_2 bubbles onto the support surface and an increasing weight due to the Pd reduction and its consequent incorporation. Fig. 10 shows the evolution of Pd external coverage deposited by ELP-PP for membranes containing 1, 2 and 3 SiO_2 dip-coating cycles (samples denoted from DC-01 to DC-03, respectively). As it can be seen, despite the previous surface analyses revealed only slight differences when 1, 2 or 3 SiO_2 layers were incorporated over the tubular PSS supports (Figs. 7 and 8), the intermediate modification has a great importance for Pd plating. In case of considering only one SiO_2 intermediate layer, the 0.2 M N_2H_4 solution could pass through the modified support without difficulty and reacted with the Pd solution, as it occurred when calcined supports were used. Therefore, a very homogeneous Pd layer was generated onto the surface from the earlier stages of the process (see images for DC-01 in Fig. 10). However, the greater roughness of this modified support, compared with the oxidized one, causes the necessity of 22 ELP-PP cycles to obtain an apparently fully dense membrane, in which the pore blockage with Pd stopped the plating reaction. In this manner, an estimated Pd thickness of around 20 µm was obtained. In the other two cases, as the SiO_2 amount in the intermediate layer increases, the plating reaction became progressively more difficult. Thus, in the case of the modified support with 2 SiO_2 dip-coating cycles, quick diffusion of N_2H_4 solution occurs from the initial stages, although the Pd film was certainly heterogeneous (sample DC-02 in Fig. 11). In fact, it was necessary to increase progressively the N_2H_4 concentration from 0.2 to 4.0 M after 10 ELP-PP cycles in order to achieve a completely dense membrane at room temperature. In this way, 43 ELP-cycles were necessary to complete the membrane preparation, estimating a final Pd thickness of around 40 µm. Finally, the chemical reaction between both hydrazine and Pd source solutions became definitively hindered in case of using a modified support with 3 dense SiO_2 cycles, as evidencing the total absence of N_2 bubbles and weight gain in the sample after the first cycles with hydrazine 0.2 M. This can be observed in the photographs taken for membrane DC-03 (Fig. 10), in which the incorporation of Pd on the external surface is nearly negligible after the first ELP-PP cycle. The reaction only started after employing a hydrazine concentration of 1.0 M during the third ELP-PP cycle, detecting heterogeneously distributed palladium along the external surface of the membrane. The plated area was progressively growing up until the reaction stopped after 41 ELP-PP cycles, estimating 39 µm of Pd thickness by gravimetric analysis.

3.3. Permeation behavior and membrane morphology after tests

Prior to analyze the permeation behavior at high temperature for

Table 2
Main parameters of the membranes studied and referred in this work.

Membrane ID	SiO_2 layers	Support calcination	ELP-PP cycles	Pd thickness (µm)*	Ref
OXI-PP	None	YES	19	11	[40]
OXI-Pd	None	YES	20	10–15	This work
DC-01-Pd	1	NO	22	20	This work
DC-02-Pd	2	NO	43	40	This work
DC-03-Pd	3	NO	41	39	This work

* Average value estimated by gravimetric analysis.

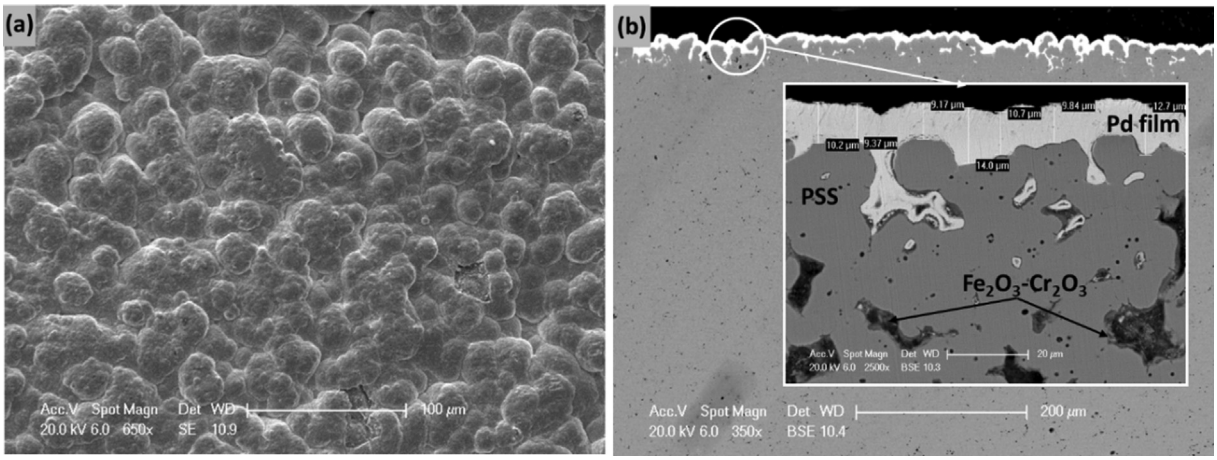

Fig. 10. SEM images of Pd membrane with Fe-Cr oxides as intermediate layer (OXI-Pd): (a) external surface and (b) cross-section.

the membranes prepared in this work, preliminary leak tests at room temperature with nitrogen were performed to ensure the continuity of the H_2-selective palladium external film. For these experiments, a permeate flux lower than $7.345{\cdot}10^{-5}$ mol m^{-2} s^{-1} was obtained at pressures up to 6 bar for all cases except the membrane prepared with 3 layers of SiO_2, hence evidencing a good gas-tightness for most of the prepared membranes. However, a persistent nitrogen leak in one of the welding areas between both porous and dense 316L SS for the mentioned membrane was observed, making the deposition of a completely dense Pd film by ELP-PP difficult and hindering its use in the present study.

After that, permeation tests with pure hydrogen and H_2-N_2 mixtures at high temperature were performed for the rest of the Pd-based membranes prepared in this work. The first membrane, including 1 layer of SiO_2 incorporated by dip-coating and the palladium film deposited by ELP-PP Membrane (DC01-Pd), underwent a rapid decrease of the ideal perm-selectivity when testing in the pilot plant at 400 °C under N_2/H_2 mixtures. Despite the previous integrity obtained under N_2 flow at room temperature, the presence of N_2 in the permeate side could be detected when testing at a higher temperature and operating pressures from 1.5 bar. Thus, the membrane was analyzed again to study possible morphological changes, collecting these results in Fig. 11. As it can be seen, a clear deterioration of the H_2-selective film was produced near the welding areas (Fig. 12a), where the Pd film was delaminated. Additionally, deep cracks along the Pd film were also detected by the SEM (Fig. 12b), contributing significantly to the membrane failure at the analyzed operating conditions. A plausible explanation can be supported by considering that an insufficient thickness of the SiO_2 intermediate layer might cause hydrazine to reach the non-porous SS surface near the welding (not previously activated), where it reacts with the Pd ions. Then, the Pd film was deposited on the welding surface, although the adherence on this surface was quite limited, compromising the resistance of the entire Pd film that could be peeled under permeation conditions. This phenomenon was not observed when using two or three layers of SiO_2 as intermediate barrier because the presence of a greater amount of ceramic particles within the PSS pores turns more difficult the hydrazine to reach the external surface. Then, it can be concluded that only one layer of SiO_2 as intermediate barrier seemed to not be adequate for the preparation of a resistant membrane by ELP-PP method.

Additionally, Fig. 13 shows the elemental mapping of the previous cross-sectional SEM image for sample DC01-Pd. As it can be seen,

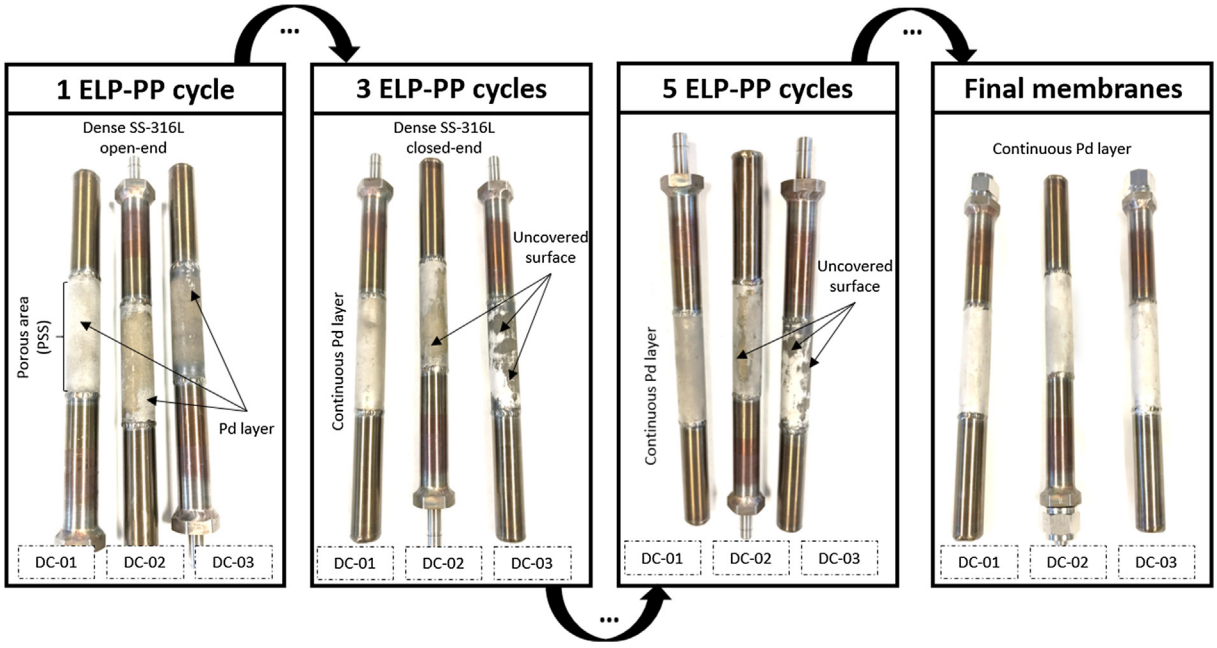

Fig. 11. Evolution of Pd-layer prepared by ELP-PP over modified PSS supports with dense SiO_2.

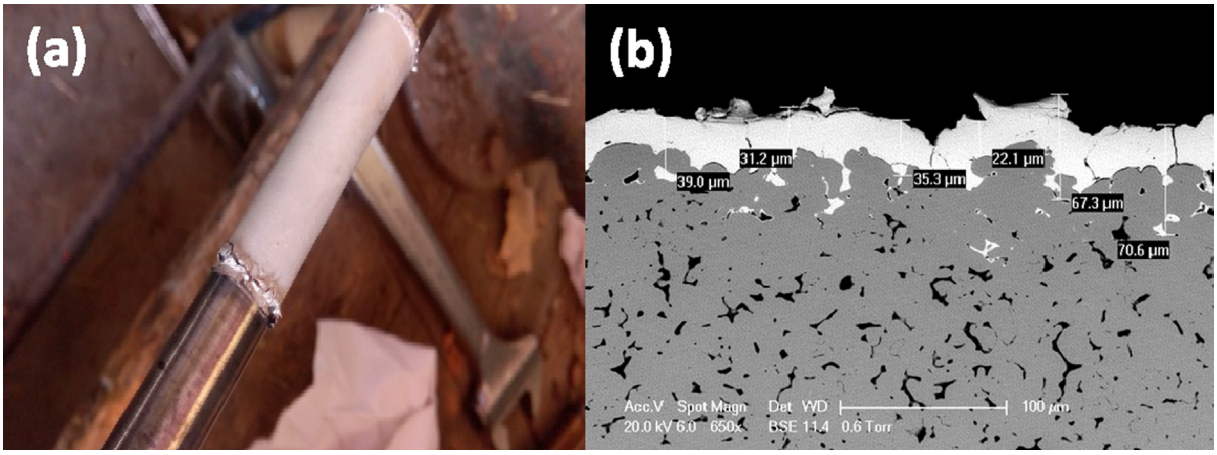

Fig. 12. Morphological analysis of the Pd-based membrane prepared with 1 SiO_2 layer (DC01-Pd) after permeation tests at high temperature (T = 400 °C): a) External photograph and b) cross-sectional SEM image.

intermetallic diffusion/migration was not observed between the support elements and the Pd film because of the adequate function of the SiO_2 particles as protective layer and/or the limited time of the experiment at high temperature. Some SiO_2 particles seem to have been dragged to the surface during the preparation of the membrane for the SEM analysis, but in general, a good coverage of the original pores of PSS support with these particles can be observed.

Fortunately, a better mechanical resistance was obtained with the membrane when 2 layers of SiO_2 are included as intermediate barrier and an external Pd film was deposited by ELP-PP (DC02-Pd). In this case, the initial H_2 perm-selectivity of the membrane remained almost constant for the whole testing period as evidencing the leak tests performed before and after each permeation test at high temperature. This membrane was tested at 400 °C and a constant pressure difference of 4 bar while using different feed compositions: pure H_2 and mixtures with a decreasing H_2 content of 70% and 50% (vol/vol). All these permeation results are presented in Fig. 14, indicating the evolution with time for both, total and H_2 permeate flowrates at mentioned diverse feed compositions.

As expected, despite maintaining a constant total pressure between both retentate and permeate sides, total and H_2 permeate flowrates decrease when H_2 contents decreases in the feed stream, because of the decreasing of the permeation driving force. The hydrogen selectivity was calculated accordingly to the eq. (2) (detailed in previous section 2), obtaining an initial value around 57, which was kept during membrane testing for more than 720 h. However, during the last operating conditions tested (50/50 H_2/N_2 % v/v) a significant reduction in selectivity was observed which indicated the starting of membrane degradation. Due to the limited value achieved during these experiments, it has been decided to analyze again the morphology of the membrane

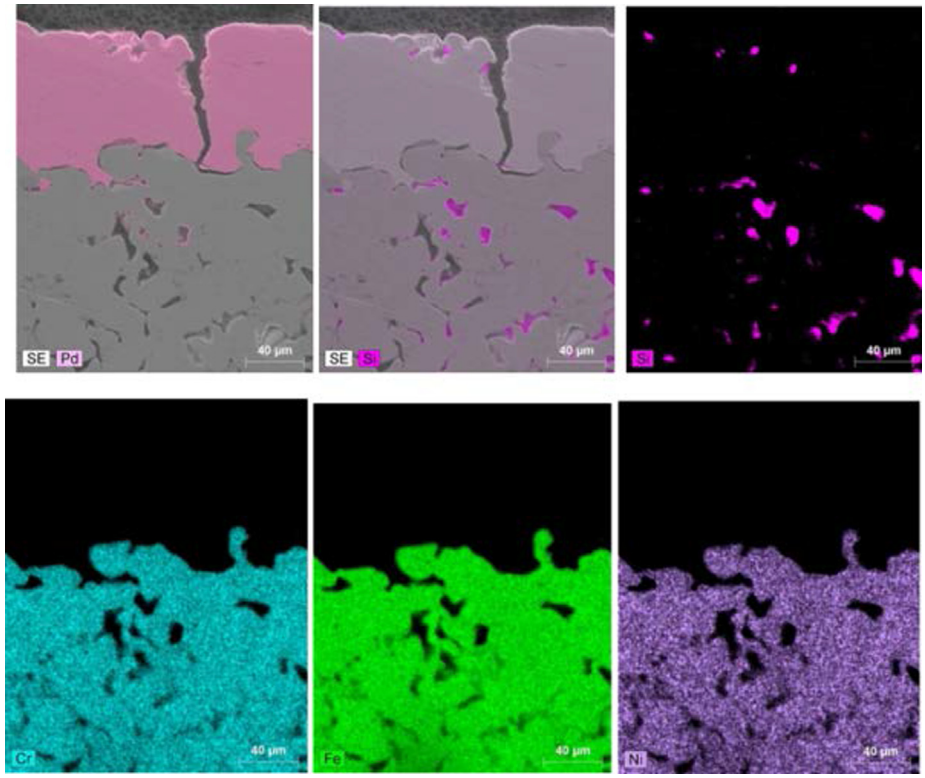

Fig. 13. Elemental EDX mapping for the cross-section of Pd-based membrane prepared with 1 SiO_2 layer (DC01-Pd) after permeation tests at high temperature (T = 400 °C).

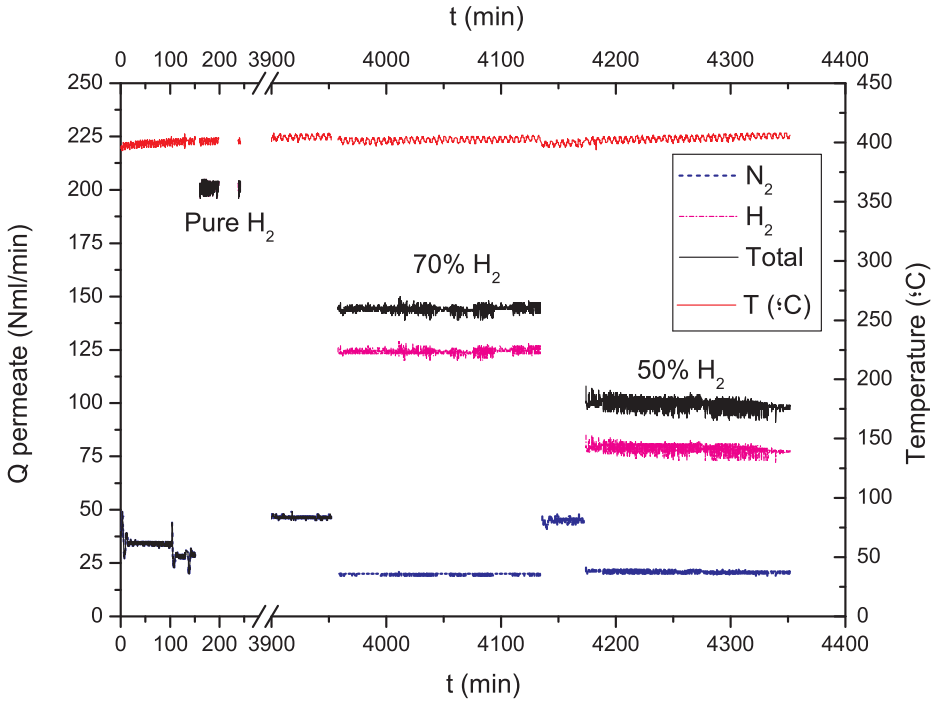

Fig. 14. Permeation behavior of membrane DC02-Pd (T = 400 °C, DP = 4 bar and total Q_{feed} = 1 NL/min).

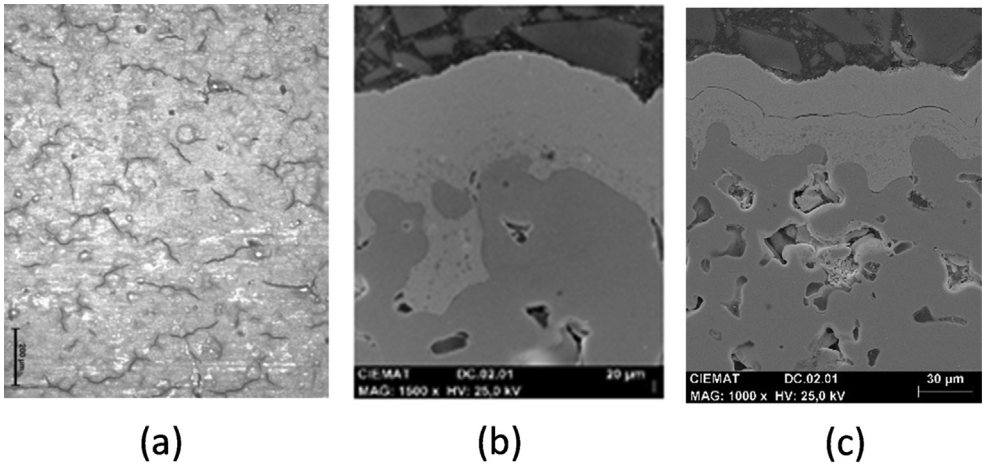

Fig. 15. Optical and SEM micrographs of membrane DC02-Pd after testing at 400 °C and pressure difference of 4 bar.

after testing. This analysis was carried out by optical and scanning electron microscopy of the external surface of the membrane DC02-Pd after testing (Fig. 15), obtaining generalized micro-cracks on the external Pd layer that could be derived from a limited thermal resistance of the interphase silica-metal (Fig. 15a, taking with an optical microscope). Cross-sectional images obtained by SEM (Fig. 15b and c) reveals that a real external Pd layer was thickness around 40 µm, very close to the estimated value from gravimetric analyses. This thick layer could also justify the limited permeation values obtained during the experiments at high temperatures, although it cannot be explain the relatively low H_2 perm-selectivity, probably due to an open porosity in the Pd film derived from the generation of cracks as previously discussed and not clearly observed in the cross-sectional images. In fact, some voids seem to be appeared in certain areas of the selective layer, suggesting a possible delamination effect after testing, but most of them are not always opened to the external surface. As previously indicated, it could be produced by the marked differences between the thermal expansion coefficients of silica and palladium, although the modification of the Pd deposition conditions could be also responsible of this effect. It means that the necessity of increasing the hydrazine concentration during the ELP-PP process from 0.2 to 4.0 M could cause a negative effect on its dosage (previously optimized for a support with relatively open porosity [27,40]) and, consequently, in the adequate adherence of the film. This hypothesis could justify in a certain way the voids and delamination observed in the cross-sectional images. Due to the current research is still in progress, additional experiments and studies are being carried out to elucidate this uncertainty.

Finally, the performance of membrane DC02-Pd presented in this work has been compared with other membranes from literature and fabricated by ELP-PP but replacing the SiO_2 intermediate barrier by another one formed by Fe-Cr oxides. Previous experience of authors showed that the generation of a Fe-Cr oxides interlayer was enough to slightly modify both original roughness and external pores of original PSS support, being possible to prepare membranes with good performance at high temperatures and pressure driving forces up to 2.5 bar [40,42]. In this work, a new membrane following this strategy was also prepared, but increasing the permeation area with a tubular PSS support welded in both extremes to dense SS and tested at higher pressures.

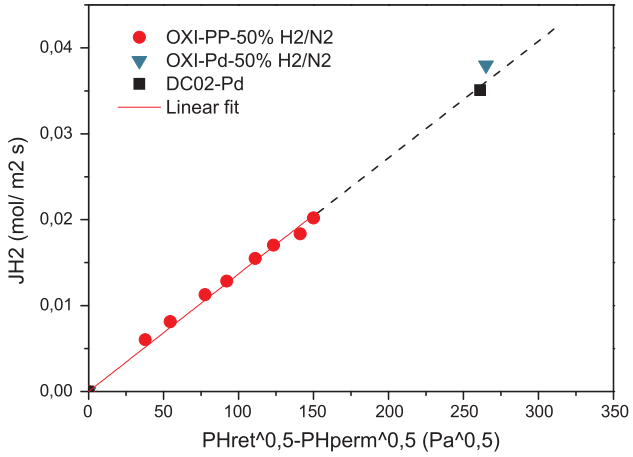

Fig. 16. Performance comparison for ELP-PP Pd-membranes containing diverse intermediate layers: SiO_2 and Fe-Cr oxides (T = 400 °C; Feed gas composition: 50% v/v H_2/N_2).

Fig. 16 depicts the results obtained for these three membranes for comparison. As it can be seen, both OXI-Pd membranes show a permeation behavior with a very similar permeance value ($1.45{\cdot}10^{-4}$ mol m^{-2} s $Pa^{-0.5}$), accordingly to the Sievertś law. It implies a good reproducibility of the ELP-PP membrane preparation method and ensures the mechanical integrity of the membrane when testing at higher pressures, despite working with longer tubular supports. In this context, the membrane DC02-Pd, including a SiO_2 instead of Fe-Cr oxides intermediate barrier, showed a very similar permeation behavior when testing at high temperature (T = 400 °C) and ΔP = 4 bar, although the real H_2 perm-selectivity is considerably lower. As it has been previously discussed, it could be due to the modification of hydrazine concentration during the ELP-PP process or the thermal compatibility between palladium and ceramic used in the intermediate barrier. Despite complementary studies are still going on to answer these questions, we consider that the results here collected have provided new interesting information about ELP-PP membranes. Some problems/limitations for the preparation of membranes by this method, especially in case of considering ceramic intermediate barriers on PSS supports, are revealed, being possible to be considered to optimize the preparation of new membranes with diverse multiple intermediate layers.

All these results have been also compared with other membranes collected from the literature. Similar membranes in terms of support material, intermediate layer and H_2-selective film composition have been considered for this comparison (see Table 3). As it can be seen, quite different permeation properties are available, although most of them show relatively high H_2 separation factors. The membrane PSS/Fe_2O_3-Cr_2O_3/Pd presented in this work exhibits a complete H_2 selectivity, but a limited permeability derived from the partial Pd deposition inside the pores of the support as discussed elsewhere [40]. However, in addition to similar results previously published [41], the membrane exhibits a good resistance to operating conditions up to ΔP = 4 bar. On the other hand, the PSS/SiO_2/Pd membrane presents similar permeation properties but limited H_2 selectivity, in spite of the high thickness of the Pd film.

4. Conclusions and future work

The influence of different approaches for tuning the surface of PSS supports prior to Pd Electroless Pore-Plating has been investigated in this work. Two different types of oxides were considered: Fe_2O_3-Cr_2O_3, generated by direct calcination, and SiO_2, deposited by dip-coating. Preliminary tests performed on planar supports evidenced that porous SiO_2 allows obtaining a continuous intermediate layer, but with a limited adherence to the PSS supporting. Much more effective was the use of dense SiO_2, which positively contributed to reduce the average support porosity and surface roughness. Based on this preliminary positive result, combination of both approaches was investigated (calcination followed by the deposition of SiO_2 by dip-coating). However, results showed that the presence of a layer of Fe/Cr oxides seemed to prevent a subsequent filling of the internal pores of the support by SiO_2 suggesting that the combination of both alternatives did not provide any evident beneficial effect on the Pd layer formation by ELP-PP method. Modification of PSS tubular supports with 1, 2 and 3 layers of dense SiO_2 were carried out, demonstrating a clear influence of the amount of silica deposited on the subsequent Pd incorporation by ELP-PP. An increasing number of SiO_2 layers was found to reduce significantly both original PSS pore size and roughness, but at the same time it made much more difficult the diffusion of hydrazine through the modified support, being necessary to increase progressively its concentration. Balancing both effects, the modified support with two SiO_2 layers was considered the most suitable for the preparation of the selective layer by ELP-PP method. This membrane exhibited H_2 permeability in the range of $5.8–8.1{\cdot}10^{-9}$ mol m^{-1} s^{-1} $Pa^{-0.5}$ with a limited selectivity to H_2 (α ≈57) at 4 bar as pressure driving force. It was also observed that SiO_2 intermediate layer protected the surface and helped to minimize the possible intermetallic diffusion between metal support and Pd film. Comparing this membrane with those prepared by direct PSS calcination and ELP-PP, similar permeability values were obtained

Table 3
Comparison of performance of membranes collected from literature.

Support	Intermediate layer	Selective layer	Deposition method	$t_{selective\ layer}$ (μm)	Permeation conditions		Permeation capacity	H_2 separation factor	Ref.
					T (°C)	ΔP (kPa)			
PSS	Al_2O_3	Pure Pd	Free-EDTA ELP	5.0	400	100	$3.05{\cdot}10^{-3}$ [a]	500	[55]
α-Al_2O_2	silitalite-1	Pure Pd	Conventional ELP	6.0	500	100	$1.95{\cdot}10^{-6}$ [b]	1165	[56]
PSS	NaA zeolite	Pure Pd	Conventional ELP	19.0–26.0	400–450	20–150	$\leq 1.12{\cdot}10^{-3}$ [a]	20–608	[53]
PSS	NaA zeolite	PdAg	Conventional ELP	20.0	400–451	100	0.01–0.12 [c]	300-∞	[57]
α -Al_2O_2	γ-Al_2O_2	Pure Pd	Modified ELP	4.5	450	100	0.16 [c]	2072	[52]
PSS	SiO_2	Pure Pd	CVD/ELP	5.0	500	50	0.14 [c]	300–450	[58]
PSS	NaX zeolite	Pd/TiO_2	DC (dip-coating)	n.a.	450	300	0.25 [c]	1025–703	[59]
PSS	Al_2O_3, SiO_2	Pd/SiO_2	DC/ELP	n.a.	350	42	$0.60–2.30{\cdot}10^{-8}$ [b]	30–115	[60]
Al_2O_2	n.a.	Pure Pd	Conventional ELP	14.0	350–450	10–60	$2.50–3.60{\cdot}10^{-6}$ [d]	∞	[42]
Al_2O_3	n.a.	Pure Pd	ELP-PP	8.0	350–451	10–60	$5.80–8.50{\cdot}10^{-7}$ [d]	> 2500	[42]
PSS	Fe_2O_3-Cr_2O_3	Pure Pd	ELP-PP	11.0–20.0	350–450	100–250	$1.00{\cdot}10^{-4}$-$6.00{\cdot}10^{-4}$ [a]	∞	[40]
PSS	Fe_2O_3-Cr_2O_3	Pure Pd	ELP-PP	11.9	400	400	$1.45{\cdot}10^{-4}$ [a]	∞	This work
PSS	SiO_2	Pure Pd	ELP-PP	20.0–40.0	400	400	$5.8–8.1{\cdot}10^{-9}$ [d]	57	This work

Permeation capacity: [a] Permeance (mol m^{-2} s^{-1} $Pa^{-0.5}$), [b] Permeance (mol m^{-2} s^{-1} Pa^{-1}), [c] Permeation flux (mol m^{-2} s^{-1}) or [d] Permeability (mol m^{-1} s^{-1} $Pa^{-0.5}$).
n.a.: non available.

but with lower perm-selectivity.

Based on the results obtained in this work it can be concluded that dip-coating technique could be considered a very promising method for tuning PSS supports, but an optimization of the technique to obtain thinner and stable ceramic layers is still required. Significant insights regarding the influence of the intermediate layer in the preparation of the Pd selective layer by ELP-PP technique suggested that optimization is needed for each type of intermediate layer. In this context, future work includes ELP-PP optimization in case of using intermediate layers with limited average pore diameters, where diffusion of the hydrazine solution turns more difficult. Moreover, other oxide materials such as modified ZrO_2 (YSZ, x-ZrO_2) and CeO_2 are being considered to mitigate the possible negative effect of the low thermal expansion coefficient of SiO_2 for these particular applications.

5. Data availability

The raw and processed data required to reproduce these findings cannot be shared at this time as the data also forms part of an ongoing study.

Declaration of Competing Interest

The authors declared that there is no conflict of interest.

Appendix A. Supplementary material

Supplementary data to this article can be found online at https://doi.org/10.1016/j.seppur.2019.116091.

References

[1] S.Z. Baykara, Hydrogen: A brief overview on its sources, production and environmental impact, Int. J. Hydrogen Energy 43 (2018) 10605–10614, https://doi.org/10.1016/j.ijhydene.2018.02.022.

[2] C.-H. Kim, J.-Y. Han, H. Lim, K.-Y. Lee, S.-K. Ryi, Methane steam reforming using a membrane reactor equipped with a Pd-based composite membrane for effective hydrogen production, Int. J. Hydrogen Energy (2017), https://doi.org/10.1016/j.ijhydene.2017.10.054.

[3] C. Coutanceau, S. Baranton, T. Audichon, Chapter 2 - Hydrogen Production From Thermal Reforming BT - Hydrogen Electrochemical Production, Hydrog. Energy Fuel Cells Prim. Academic Press, 2018, pp. 7–15, , https://doi.org/10.1016/B978-0-12-811250-2.00002-9.

[4] E. Kniaginicheva, N. Pismenskaya, S. Melnikov, E. Belashova, P. Sistat, M. Cretin, V. Nikonenko, Water splitting at an anion-exchange membrane as studied by impedance spectroscopy, J. Memb. Sci. 496 (2015) 78–83, https://doi.org/10.1016/j.memsci.2015.07.050.

[5] A. Valente, D. Iribarren, J. Dufour, Harmonised life-cycle global warming impact of renewable hydrogen, J. Clean. Prod. 149 (2017) 762–772, https://doi.org/10.1016/j.jclepro.2017.02.163.

[6] A.M. Abdalla, S. Hossain, O.B. Nisfindy, A.T. Azad, M. Dawood, A.K. Azad, Hydrogen production, storage, transportation and key challenges with applications: A review, Energy Convers. Manag. 165 (2018) 602–627, https://doi.org/10.1016/j.enconman.2018.03.088.

[7] P. Li, Z. Wang, Z. Qiao, Y. Liu, X. Cao, W. Li, J. Wang, S. Wang, Recent developments in membranes for efficient hydrogen purification, J. Memb. Sci. 495 (2015) 130–168, https://doi.org/10.1016/j.memsci.2015.08.010.

[8] A. Arratibel Plazaola, D. Pacheco Tanaka, M. Van Sint Annaland, F. Gallucci, Recent advances in Pd-based membranes for membrane reactors, Molecules 22 (2017) 51, https://doi.org/10.3390/molecules22010051.

[9] D. Alique, D. Martinez-Diaz, R. Sanz, J.A. Calles, Review of supported pd-based membranes preparation by electroless plating for ultra-pure hydrogen production, Membranes (2018), https://doi.org/10.3390/membranes8010005.

[10] J.J. Conde, M. Maroño, J.M. Sánchez-Hervás, Pd-based membranes for hydrogen separation: review of alloying elements and their influence on membrane properties, Sep. Purif. Rev. 46 (2017) 152–177, https://doi.org/10.1080/15422119.2016.1212379.

[11] J.M. Sánchez, M.M. Barreiro, M. Maroño, Hydrogen enrichment and separation from synthesis gas by the use of a membrane reactor, Biomass Bioenergy 35 (2011), https://doi.org/10.1016/j.biombioe.2011.03.037.

[12] Advanced Hydrogen Transport Membranes for Coal Gasification, (n.d.). https://www.netl.doe.gov/.

[13] G. Di Marcoberardino, M. Binotti, G. Manzolini, J.L. Viviente, A. Arratibel, L. Roses, F. Gallucci, Achievements of European projects on membrane reactor for hydrogen production, J. Clean. Prod. 161 (2017) 1442–1450, https://doi.org/10.1016/j.jclepro.2017.05.122.

[14] E. Fernandez, A. Helmi, J.A. Medrano, K. Coenen, A. Arratibel, J. Melendez, N.C.A. de Nooijer, V. Spallina, J.L. Viviente, J. Zuñiga, M. van Sint Annaland, D.A. Pacheco Tanaka, F. Gallucci, Palladium based membranes and membrane reactors for hydrogen production and purification: An overview of research activities at Tecnalia and TU/e, Int. J. Hydrogen Energy. 42 (2017) 13763–13776, https://doi.org/10.1016/j.ijhydene.2017.03.067.

[15] C. Zhao, H. Xu, A. Goldbach, Duplex Pd/ceramic/Pd composite membrane for sweep gas-enhanced CO_2 capture, J. Memb. Sci. 563 (2018) 388–397, https://doi.org/10.1016/j.memsci.2018.05.057.

[16] A.M. Tarditi, M.L. Bosko, L.M. Cornaglia, Electroless plating of Pd binary and ternary alloys and surface characteristics for application in hydrogen separation, Elsevier, Oxford, 2017, pp. 1–24, https://doi.org/10.1016/B978-0-12-803581-8.09166-9.

[17] M.R. Rahimpour, F. Samimi, A. Babapoor, T. Tohidian, S. Mohebi, Palladium membranes applications in reaction systems for hydrogen separation and purification: A review, Chem. Eng. Process. Process Intensif. 121 (2017) 24–49, https://doi.org/10.1016/j.cep.2017.07.021.

[18] A. Arratibel, J.A. Medrano, J. Melendez, D.A. Pacheco Tanaka, M. van Sint Annaland, F. Gallucci, Attrition-resistant membranes for fluidized-bed membrane reactors: Double-skin membranes, J. Memb. Sci. 563 (2018) 419–426, https://doi.org/10.1016/j.memsci.2018.06.012.

[19] J. Melendez, E. Fernandez, F. Gallucci, M. van Sint Annaland, P.L. Arias, D.A.P. Tanaka, Preparation and characterization of ceramic supported ultra-thin (~1 μm) Pd-Ag membranes, J. Memb. Sci. 528 (2017) 12–23, https://doi.org/10.1016/j.memsci.2017.01.011.

[20] D.A.P. Tanaka, J. Okazaki, M.A.L. Tanco, T.M. Suzuki, 5 - Fabrication of supported palladium alloy membranes using electroless plating techniques, in: A. Doukelis, K. Panopoulos, A. Koumanakos, E. Kakaras (Eds.), Palladium Membr. Technol. Hydrog. Prod. Carbon Capture Other Appl. Woodhead Publishing, 2015, pp. 83–99, , https://doi.org/10.1533/9781782422419.1.83.

[21] F. Guazzone, Engineering of substrate surface for the synthesis of UltraThin composite Pd and Pd-Cu membranes for H_2 separation, Worcester Polytechnic Institute, 2005.

[22] J.A. Calles, R. Sanz, D. Alique, Influence of the type of siliceous material used as intermediate layer in the preparation of hydrogen selective palladium composite membranes over a porous stainless steel support, Int. J. Hydrogen Energy 37 (2012) 6030–6042, https://doi.org/10.1016/j.ijhydene.2011.12.164.

[23] T. Van Gestel, F. Hauler, M. Bram, W.A. Meulenberg, H.P. Buchkremer, T. Van Gestel, F. Hauler, M. Bram, W.A. Meulenberg, H.P. Buchkremer, Synthesis and characterization of hydrogen-selective sol–gel SiO_2 membranes supported on ceramic and stainless steel supports, Sep. Purif. Technol. 121 (2014) 20–29, https://doi.org/10.1016/j.seppur.2013.10.035.

[24] D. Alique, Processing and characterization of coating and thin film materials, in: J. Zhang, Y. Jung (Eds.), Adv. Ceram. Met. Coat. Thin Film Mater. Energy Environ. 2018, https://doi.org/10.1007/978-3-319-59906-9.

[25] I.P. Mardilovich, E. Engwall, Y.H. Ma, Dependence of hydrogen flux on the pore size and plating surface topology of asymmetric Pd-porous stainless steel membranes, Desalination 144 (2002) 85–89, https://doi.org/10.1016/S0011-9164(02)00293-X.

[26] Y. Huang, R. Dittmeyer, Preparation of thin palladium membranes on a porous support with rough surface, J. Memb. Sci. 302 (2007) 160–170, https://doi.org/10.1016/j.memsci.2007.06.040.

[27] L. Furones, D. Alique, Interlayer properties of in-situ oxidized porous stainless steel for preparation of composite Pd membranes, ChemEng. 2 (2017) 1, https://doi.org/10.3390/chemengineering2010001.

[28] A. Tarditi, C. Gerboni, L. Cornaglia, PdAu membranes supported on top of vacuum-assisted ZrO2-modified porous stainless steel substrates, J. Memb. Sci. 428 (2013) 1–10, https://doi.org/10.1016/j.memsci.2012.10.029.

[29] H.W.A. El Hawa, S.-T.B. Lundin, N.S. Patki, J.D. Way, Steam methane reforming in a PdAu membrane reactor: Long-term assessment, Int. J. Hydrogen Energy 41 (2016) 10193–10201, https://doi.org/10.1016/j.ijhydene.2016.04.244.

[30] A. Ayral, Others, silica membranes - basic principles, Period. Polytech. Ser. Chem. Eng. 50 (2006) 67–79.

[31] S.-E. Nam, K.-H. Lee, Hydrogen separation by Pd alloy composite membranes: introduction of diffusion barrier, J. Memb. Sci. 192 (2001) 177–185, https://doi.org/10.1016/S0376-7388(01)00499-9.

[32] L. Zheng, H. Li, T. Xu, F. Bao, H. Xu, Defect size analysis approach combined with silicate gel/ceramic particles for defect repair of Pd composite membranes, Int. J. Hydrogen Energy 41 (2016) 18522–18532, https://doi.org/10.1016/j.ijhydene.2016.08.169.

[33] M. Kanezashi, D. Fuchigami, T. Yoshioka, T. Tsuru, Control of Pd dispersion in sol–gel-derived amorphous silica membranes for hydrogen separation at high temperatures, J. Memb. Sci. 439 (2013) 78–86, https://doi.org/10.1016/j.memsci.2013.03.037.

[34] S.H. Chaki, M.P. Deshpande, J.P. Tailor, Characterization of CuS nanocrystalline thin films synthesized by chemical bath deposition and dip coating techniques, Thin Solid Films 550 (2014) 291–297, https://doi.org/10.1016/j.tsf.2013.11.037.

[35] D.B. Mitzi (Ed.), Solution processing of inorganic materials, John Willey and Sons Inc, 2008, , https://doi.org/10.1002/9780470407790.

[36] A. Morales, Process to deposit metal and metal oxides, European Patent 1321539, 2001.

[37] A. Arratibel, D.A. Pacheco Tanaka, T.J.A. Slater, T.L. Burnett, M. van Sint Annaland, F. Gallucci, Unravelling the transport mechanism of pore-filled membranes for hydrogen separation, Sep. Purif. Technol. 203 (2018) 41–47, https://doi.org/10.1016/j.seppur.2018.04.016.

[38] S.-K. Ryi, S.-W. Lee, D.-K. Oh, B.-S. Seo, J.-W. Park, J.-S. Park, D.-W. Lee, S.S. Kim, Electroless plating of Pd after shielding the bottom of planar porous stainless steel

for a highly stable hydrogen selective membrane, J. Memb. Sci. 467 (2014) 93–99, https://doi.org/10.1016/j.memsci.2014.04.058.
[39] G.O. Mallory, J.B. Hajdu, Electroless plating: fundamentals and applications, American Electroplaters and Surface Finishers Society, 1990.
[40] R. Sanz, J.A. Calles, D. Alique, L. Furones, New synthesis method of Pd membranes over tubular PSS supports via "pore-plating" for hydrogen separation processes, Int. J. Hydrogen Energy 37 (2012) 18476–18485, https://doi.org/10.1016/j.ijhydene.2012.09.084.
[41] J.A. Calles, R. Sanz, D. Alique, L. Furones, P. Marín, S. Ordoñez, Influence of the selective layer morphology on the permeation properties for Pd-PSS composite membranes prepared by electroless pore-plating: Experimental and modeling study, Sep. Purif. Technol. 194 (2018) 10–18, https://doi.org/10.1016/j.seppur.2017.11.014.
[42] D. Alique, M. Imperatore, R. Sanz, J.A. Calles, M.G. Baschetti, Hydrogen permeation in composite Pd-membranes prepared by conventional electroless plating and electroless pore-plating alternatives over ceramic and metallic supports, Int. J. Hydrogen Energy 41 (2016) 19430–19438, https://doi.org/10.1016/j.ijhydene.2016.06.128.
[43] A. Morales, Sol-gel process to the preparation of porous coatings, using precursor solutions prepared by polymeric reactions, European Patent 1329433, 2001.
[44] F. Guazzone, Y.H. Ma, Leak growth mechanism in composite Pd membranes prepared by the electroless deposition method, AIChE J. 54 (2008), https://doi.org/10.1002/aic.
[45] M.M. Barreiro, M. Maroño, J.M. Sánchez, Hydrogen separation studies in a membrane reactor system: Influence of feed gas flow rate, temperature and concentration of the feed gases on hydrogen permeation, Appl. Therm. Eng. 74 (2015) 186–193, https://doi.org/10.1016/j.applthermaleng.2013.12.035.
[46] M.M. Barreiro, M. Maroño, J.M. Sánchez, Hydrogen permeation through a Pd-based membrane and RWGS conversion in H_2/CO_2, $H_2/N_2/CO_2$ and $H_2/H_2O/CO_2$ mixtures, Int. J. Hydrogen Energy 39 (2014) 4710–4716, https://doi.org/10.1016/j.ijhydene.2013.11.089.
[47] S. Yun, S. Ted Oyama, Correlations in palladium membranes for hydrogen separation: A review, J. Memb. Sci. 375 (2011) 28–45, https://doi.org/10.1016/j.memsci.2011.03.057.
[48] C.-B. Lee, S.-W. Lee, J.-S. Park, S.-K. Ryi, D.-W. Lee, K.-R. Hwang, S.-H. Kim, Ceramics used as intermetallic diffusion barriers in Pd-based composite membranes sputtered on porous nickel supports, J. Alloys Compd. 578 (2013) 425–430, https://doi.org/10.1016/j.jallcom.2013.06.007.
[49] D. Alique, M. Imperatore, R. Sanz, J.A. Calles, M. Giacinti Baschetti, Hydrogen permeation in composite Pd-membranes prepared by conventional electroless plating and electroless pore-plating alternatives over ceramic and metallic supports, Int. J. Hydrogen Energy 41 (2016) 19430–19438, https://doi.org/10.1016/j.ijhydene.2016.06.128.
[50] J.A. Calles, R. Sanz, D. Alique, L. Furones, Thermal stability and effect of typical water gas shift reactant composition on H_2 permeability through a Pd-YSZ-PSS composite membrane, Int. J. Hydrogen Energy. 39 (2014) 1398–1409, https://doi.org/10.1016/j.ijhydene.2013.10.168.
[51] R. Sanz, J.A. Calles, S. Ordóñez, P. Marín, D. Alique, L. Furones, Modelling and simulation of permeation behaviour on Pd/PSS composite membranes prepared by "pore-plating" method, J. Memb. Sci. 446 (2013) 410–421, https://doi.org/10.1016/j.memsci.2013.06.060.
[52] L. Zheng, H. Li, H. Xu, "Defect-free" interlayer with a smooth surface and controlled pore-mouth size for thin and thermally stable Pd composite membranes, Int. J. Hydrogen Energy 41 (2016) 1002–1009, https://doi.org/10.1016/j.ijhydene.2015.09.024.
[53] M.L. Bosko, F. Ojeda, E.A. Lombardo, L.M. Cornaglia, NaA zeolite as an effective diffusion barrier in composite Pd/PSS membranes, J. Memb. Sci. 331 (2009) 57–65, https://doi.org/10.1016/j.memsci.2009.01.005.
[54] D.A. Pacheco Tanaka, M.A. Llosa Tanco, T. Nagase, J. Okazaki, Y. Wakui, F. Mizukami, T.M. Suzuki, Fabrication of hydrogen-permeable composite membranes packed with palladium nanoparticles, Adv. Mater. 18 (2006) 630–632, https://doi.org/10.1002/adma.200501900.
[55] S.K. Gade, P.M. Thoen, J.D. Way, Unsupported palladium alloy foil membranes fabricated by electroless plating, J. Memb. Sci. 316 (2008) 112–118, https://doi.org/10.1016/j.memsci.2007.08.022.
[56] Y. Guo, Y. Jin, H. Wu, L. Zhou, Q. Chen, X. Zhang, X. Li, Preparation of palladium membrane on Pd/silicalite-1 zeolite particles modified macroporous alumina substrate for hydrogen separation, Int. J. Hydrogen Energy. 39 (2014) 21044–21052, https://doi.org/10.1016/j.ijhydene.2014.10.089.
[57] M.L. Bosko, J.F. Múnera, E.A. Lombardo, L.M. Cornaglia, Dry reforming of methane in membrane reactors using Pd and Pd-Ag composite membranes on a NaA zeolite modified porous stainless steel support, J. Memb. Sci. 364 (2010) 17–26, https://doi.org/10.1016/j.memsci.2010.07.039.
[58] Y. Matsumura, T. Yazawa, Su Caili, Tetsuro Jin, Koji Kuraoka, Thin palladium film supported on SiO_2-modified porous stainless steel for a high-hydrogen-flux membrane, Ind. Eng. Chem. Res. 44 (2005) 3053–3058.
[59] M. Dehghani Mobarake, P. Jafari, M. Irani, Preparation of Pd-based membranes on Pd/TiO_2 modified NaX/PSS substrate for hydrogen separation: Design and optimization, Microporous Mesoporous Mater. 226 (2016) 369–377, https://doi.org/10.1016/j.micromeso.2016.02.022.
[60] D. Lee, C. Yu, K. Lee, Synthesis of Pd particle-deposited microporous silica membranes via a vacuum-impregnation method and their gas permeation behavior, J. Colloid Interface Sci. 325 (2008) 447–452, https://doi.org/10.1016/j.jcis.2008.06.021.